

Excitation rate dependence of Auger recombination in silicon

Patrick E. Hopkins, Edward V. Barnat, Jose L. Cruz-Campa, Robert K. Grubbs, Murat Okandan et al.

Citation: *J. Appl. Phys.* **107**, 053713 (2010); doi: 10.1063/1.3309759

View online: <http://dx.doi.org/10.1063/1.3309759>

View Table of Contents: <http://jap.aip.org/resource/1/JAPIAU/v107/i5>

Published by the [American Institute of Physics](#).

Additional information on *J. Appl. Phys.*

Journal Homepage: <http://jap.aip.org/>

Journal Information: http://jap.aip.org/about/about_the_journal

Top downloads: http://jap.aip.org/features/most_downloaded

Information for Authors: <http://jap.aip.org/authors>

ADVERTISEMENT



AIPAdvances

Now Indexed in
Thomson Reuters
Databases

Explore AIP's open access journal:

- Rapid publication
- Article-level metrics
- Post-publication rating and commenting

Excitation rate dependence of Auger recombination in silicon

Patrick E. Hopkins,^{a)} Edward V. Barnat, Jose L. Cruz-Campa, Robert K. Grubbs, Murat Okandan, and Gregory N. Nielson
Sandia National Laboratories, Albuquerque, New Mexico 87123, USA

(Received 14 October 2009; accepted 12 January 2010; published online 5 March 2010)

This work reports on measurements of the Auger recombination coefficients in silicon wafers with pump-probe thermoreflectance techniques operating at two different excitation rates: 250 kHz (low repetition rate) and 80 MHz (high repetition rate). The different excitation frequencies give rise to different thermoreflectance signals in the Si samples, which is ascribed to the excited number density in the conduction band. In the low repetition rate case, the excited carriers recombine via Auger processes before the next pump excitation is absorbed. However, in the high repetition rate case, the rate in which the pump excitations are absorbed at the sample surface is higher than the Auger recombination rate, indicating that the excited carrier densities in the high repetition rate experiments are much higher than in the low repetition rate measurements even though the pump fluences are comparable. This is ascribed to pulse accumulation in the high repetition rate measurements, and is quantified with rate equation and thermoreflectance models fit to the experimental data. Comparing the data taken at the two different excitation modulations gives insight into the excited carrier density when recombination rate are on the same order as excitation frequencies. © 2010 American Institute of Physics. [doi:10.1063/1.3309759]

I. INTRODUCTION

Pump-probe optical techniques for semiconductor characterization are invaluable tools for directly probing the dynamics of photoexcited carriers in semiconductor structures during nonequilibrium, nonradiative, and recombinatory processes in the time domain.¹ The use of ultrashort, subpicosecond laser pulses in pump-probe spectroscopy has led to enormous progress in understanding the basic relaxation mechanism of carriers in semiconductors.^{1,2} The recent advances in miniaturization of semiconductor-based devices along with materials processing requirements—such as surface coatings, implantation, and annealing—have a tremendous impact on the carrier dynamics and relaxation in these materials, making femtosecond optical experiments appealing techniques for measuring a wide range of excited carrier phenomena due to the time scales of the electronic relaxation mechanisms.^{3–13}

Following optical excitation, the electrons and holes undergo spatial and temporal evolution with characteristic times dependent on the various relaxation processes.¹⁴ In silicon, the first few picoseconds after optical excitation are dominated by free carrier redistribution via electron and phonon scattering and interband transitions (dominated in Si by state filling).⁵ Due to the nature of the electronic transitions, the temporal overlap of these various electronic relaxation events can give very complicated thermoreflectance signals in semiconductors (and metals alike).^{5,11,15,16} The next 100 ps–1 ns is dominated by various surface carrier recombination processes^{3,10,13} competing with recombinatory processes in the bulk of the material. Typically, the surface recombination processes are much faster than the bulk due to the high

carrier densities near the surface (i.e., closer to the excitation);² due to these high densities, these surface processes are a critical parameter in device design and optimization, specifically in optoelectronic and photovoltaic devices. In this work, we measure the Auger recombination coefficient in surface treated Si wafers with pump-probe thermoreflectance techniques of varying wavelengths and different excitation rates. The different excitation frequencies give rise to drastically different thermoreflectance signals in the Si samples, which is ascribed to the excited number density in the conduction band. We consider excitation regimes in this work ($\geq 5 \times 10^{17} \text{ cm}^{-3}$) in which Auger processes dominate excited carrier recombination.^{13,17}

As pointed out by Sabbah and Riffe,¹⁰ pump-probe techniques using above-band-gap energies for the pump and probe pulses are extremely sensitive to surface dynamics. Although the pump pulse can have a relatively large excitation depth $\delta_e \approx \lambda / (4\pi k)$, where λ is the wavelength of the pump pulse and k is the extinction coefficient ($\delta_e = 8.92 \mu\text{m}$ in Si at 785 nm incident pump wavelength), the probe pulse has a relatively small penetration depth since the pulse arrives at the sample surface after the pump has excited the carriers to the conduction band. This probe penetration depth can be estimated as $\delta_p \approx \lambda / (4\pi n)$,¹⁷ where n is the real component of the refractive index ($\delta_p = 17 \text{ nm}$ in Si at 785 nm incident pump wavelength), which is relatively small, so the probe thermoreflectance is dominated by surface carrier dynamics. Note that for optically excited semiconductors, the complex dielectric function $\hat{\epsilon} = \epsilon_1 + i\epsilon_2$ becomes dominated by ϵ_2 since ϵ_1 (ϵ_2) decreases (increases) with excited carrier density. Since the complex index of refraction is given by $\hat{n} = n + ik = \sqrt{\hat{\epsilon}}$, after pump excitation of carriers from the valence band to the conduction band, $\hat{n} \approx (1+i)\sqrt{\epsilon_2/2}$.

Since the surface carrier dynamics are governed by the

^{a)} Author to whom correspondence should be addressed. Electronic mail: pehopki@sandia.gov.

carrier number density in the conduction band, we examine the carrier dynamics with two different pump excitation frequencies, 80 MHz and 250 kHz. Given that bulk Auger recombination time of excited carriers in Si after short pulse laser absorption is on the order of 1 μ s for moderate laser fluences,¹³ the measurements taken with the 80 MHz system inhibit Auger recombination by continually pumping carriers into the conduction band, where the measurements taken with the 250 kHz system study the carrier dynamics after excitation of an Auger recombined Si surface (an excited carrier density of $N_e = 10^{18}$ cm⁻³ corresponds to an incident laser pulse of 3.4 J m⁻² at 785 nm, which equates to a bulk Auger recombination time of 2.6 μ s assuming an Auger recombination coefficient of 3.8×10^{-31} cm⁶ s⁻¹).^{2,18}

II. EXPERIMENTAL DETAILS

We probed the surface dynamics of four different Si samples. The samples were prepared from (100) oriented, p-type (boron) silicon wafers from Pure Wafer Inc. with a resistivity of 1–100 Ω cm (dopant levels of 10^{14} – 10^{16} cm⁻³). Atomic layer deposition (ALD) was used to deposit specific thicknesses of alumina on the surface of the wafers using controlled pulses of electronic grade trimethyl aluminum and water in a custom designed ALD viscous flow reactor at Sandia National Laboratories. ALD is a deposition technique that provides high conformity and thickness control by utilizing self-limiting surface reactions and sequential reactant injection.¹⁹ The samples contained \sim 2.1 nm of native oxide which was not removed before the deposition of alumina. A nitrogen carrier gas was flowed at 200 SCCM (SCCM denotes cubic centimeter per minute at STP) into the reactor to transport the chemical reactants down the hot wall reactor tube and past the samples. The depositions were performed in a temperature range of 173–190 $^{\circ}$ C and a reactor pressure of 1.0 Torr. Pulse and purge times for the reactants were identical and were 1 and 15 s, respectively. This sequence resulted in reactant pressure transients of 90 mTorr for the trimethyl aluminum and 120 mTorr for water. Running 770 ALD cycles resulted in 79 nm of ALD alumina as measured with spectroscopic ellipsometry. This resulted in a growth rate of \sim 0.1 nm per ALD cycle. After the deposition of alumina, some of the samples were annealed in hydrogen gas without an air break and various Si samples underwent different *in situ* anneals in forming gas. The forming gas anneals were performed using 25 Torr of H₂ in the reactor with a balance of N₂ to obtain a total pressure of 510 Torr in the reactor. The furnace temperature was increased to bring the reactor annealing temperature to 430 $^{\circ}$ C. Surface preparation details of the specific samples examined in this study are described in Table I.

Experimental data were taken with two different Ti:sapphire based pump-probe transient thermorefectance (TTR) setups. The high repetition rate setup is described in detail by Hopkins *et al.*,²⁰ in which the primary output emanates from a Ti:Al₂O₃ oscillator with a central wavelength of 785 nm, pulse width of \sim 90 fs with \sim 10 nJ per pulse, and a repetition rate of 80 MHz. The pump beam is modulated with an electro-optic modulator (EOM) at 11 MHz and the pump and

TABLE I. Surface preparation details of the samples examined in this study.

Sample ID	Description
α	No preheat step, 72.9 nm of alumina grown at 173 $^{\circ}$ C, and no further anneal
B	Preheat step at 430 in nitrogen, cool down, 74.6 nm of alumina grown at 190 $^{\circ}$ C, and <i>in situ</i> anneal in forming gas at 430 $^{\circ}$ C for 30 min.
AD	No preheat step, 74.6 nm of alumina grown at 190 $^{\circ}$ C, and <i>in situ</i> anneal in forming gas at 430 $^{\circ}$ C for 30 min
CE	No preheat step, 74.6 nm of alumina grown at 190 $^{\circ}$ C, with no further anneal.

probe beams are focused down to the sample surface with radii of \sim 15 μ m. The EOM broadens the pump pulse to \sim 200 fs. The low repetition rate system is based on a laser system in which the primary output emanates from a Ti:Al₂O₃ oscillator seeding a regenerative amplifier producing 200 fs pulses at 800 nm with nearly 4 μ J per pulse at 250 kHz repetition rate. The relatively energetic pulses are then split into two paths; one path is frequency doubled (pump) and the other is passed through a sapphire window to generate a white light continuum (probe).^{9,15,21} The frequency doubled 400 nm train of pump pulses are then modulated with a mechanical chopper at a repetition rate of 1 kHz and focused onto the sample surface at \sim 3 J m⁻² incident fluence. The white light probe pulses are reflected off the sample surface, passed through a bandpass filter of \sim 3 nm bandwidth centered at the wavelength of interest, and the reflectance is monitored with a photomultiplier tube. The raw data from each experimental setup were adjusted to account for experimental noise by the phase correction technique discussed by Stevens *et al.*²²

Figure 1(a) shows the phase corrected thermorefectance data (ΔR) taken on the four Si surface treated samples from the low repetition rate technique (250 kHz) at 400 nm pump and 750 nm probe wavelengths. This pump excitation corresponds to an excited carrier density of $N_e \sim 5 \times 10^{19}$ cm⁻³. Normalizing at the peak, the decay of the TTR signals over 200 ps after the peak reflectance of the four samples are nearly identical. This indicates that the surface recombination rates (to be quantified later) are identical for each of Si surface treated samples. To solidify this conclusion about the carrier dynamics at the surfaces of the four Si samples, TTR data are taken at different probe wavelengths (600, 650, 700, and 750 nm) and show nearly identical decay rates at the different wavelengths, as shown in Fig. 1(b) for the (CE) sample. The inset of Fig. 1(b) shows the maximum thermorefectance signal measured on each sample and each wavelength. Therefore, there are two important observations to note from this inset: (1) the thermorefectance signal increases as the probe wavelength (energy) increases (decreases). This is expected as the probe energy approaches the band gap of silicon and explains the increased noise in the data as probing wavelength becomes further away from the 1107 nm (1.12 eV) band gap; and (2) there is a slight variability in the magnitude of ΔR among the samples indicating that the surface treatment changed the band structure near the surface enough to effect thermorefectance, but not enough to

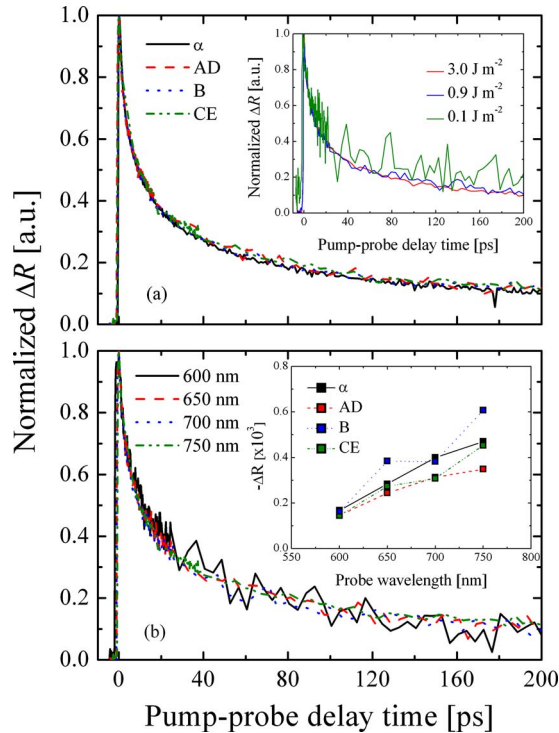


FIG. 1. (Color online) (a) ΔR from the four Si surface treated samples from the low repetition rate technique (250 kHz) at 400 nm pump and 750 nm probe wavelengths. This pump excitation corresponds to an excited carrier density of $N_e \sim 5 \times 10^{19} \text{ cm}^{-3}$. (inset) ΔR from sample B with three different incident pump fluences of 3.0, 0.9, and 0.1 J m^{-2} , corresponding to excitation number densities from 5×10^{19} – $1 \times 10^{18} \text{ cm}^{-3}$. The similar thermoreflectance responses at the three different excitation number densities indicate that Auger recombination is dominating the temporal decay on the Si samples. (b) ΔR taken at different probe wavelengths (600, 650, 700, and 750 nm), which show nearly identical decay rates at the different wavelengths. (inset) Maximum thermoreflectance signal measured on each sample and each wavelength.

change any of the carrier dynamics since the decay rates are all nearly identical. To test the effect of excited number density on the thermoreflectance response using the low repetition rate technique, we vary the incident pump fluence over an order of magnitude. The inset of Fig. 1(a) shows the thermoreflectance decay of sample B at a probe wavelength of 800 nm using incident pump fluences of 3.0, 0.9, and 0.1 J m^{-2} ; this corresponds to excitation number densities from 1×10^{18} – $5 \times 10^{19} \text{ cm}^{-3}$. Although the magnitude of the signal to noise decreases as the fluence decreases, the different fluences all exhibit the same rate of thermoreflectance decay. As previously mentioned, the thermoreflectance decay is expected to be dominated by Auger recombination. If lowering the excitation number density were to change the dominant recombinatory mechanism, then we would expect a change in the thermoreflectance decay. The similar measured temporal decays indicate that the thermoreflectance decay mechanisms at the three different excitation densities are all similarly dominated by Auger recombination.

Due to the relatively short Auger recombination time in Si compared to the time between pulses in the low repetition rate setup (4 μs), the pump effectively excites an Auger recombined Si surface. However, the high repetition rate setup operating at 80 MHz excites the sample with pump

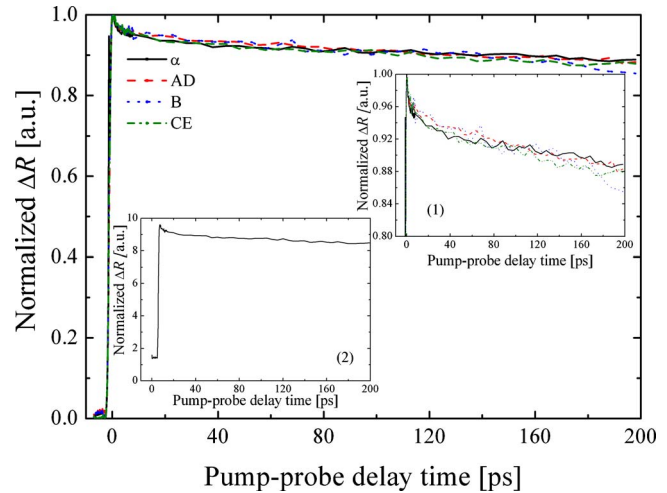


FIG. 2. (Color online) ΔR from the four different Si samples at 785 nm from the high repetition rate technique (80 MHz). Over the 200 ps delay, ΔR only relaxes down to $\sim 90\%$ of the peak value, where the data shown in Fig. 1 relax to $\sim 10\%$ of the peak value. The high repetition rate system does not allow carriers to leave (via recombination) the conduction band and, therefore, N_e is higher over a longer pump-probe delay in the high repetition rate setup. (inset 1) Thermoreflectance data on a smaller ΔR scale to see the magnitude of the decay over 200 ps more clearly. (inset 2) Representative noncorrected data set from the high repetition rate experiment. Note the nonzero value of ΔR before $t=0$ pump-probe delay time indicating accumulation of the excited number density.

pulses every 12 ns. Therefore excitation events occur before the Si system has time relax via Auger recombination. This causes drastically different reflectivity decays, as seen in Fig. 2, which plot the temporal thermoreflectance response of the four different Si samples at 785 nm. In these high repetition rate measurements, the incident pump excitation of $\sim 2 \text{ J m}^{-2}$ corresponds to an excited carrier density of $N_e \sim 6.0 \times 10^{17} \text{ cm}^{-3}$ per pump pulse. Note that this excitation number density is similar to the lowest fluence excitation in the low repetition rate experiment shown in the inset of Fig. 1(a) ($\sim 1 \times 10^{18} \text{ cm}^{-3}$). One stark difference is the fact that over the 200 ps delay, ΔR only relaxes down to $\sim 90\%$ of the peak value (seen more clearly in inset 1 of Fig. 2), where the data shown in Fig. 1 relax to $\sim 10\%$ of the peak value. Given that the thermoreflectance signal is proportional to the number of excited carriers N_e , this is intuitive since the high repetition rate system does not allow carriers to “leave” (via recombination) the conduction band, and therefore N_e is higher over a longer pump-probe delay in the high repetition rate setup.

III. EXCITED NUMBER DENSITY AND PULSE ACCUMULATION EFFECTS

To quantify the surface dynamics with the thermoreflectance data, we must determine how the excited carrier number density changes with time. In this approach, we consider ambipolar diffusion negligible in the probed region over the time scale of interest so that the excited number density balance equation becomes

$$\frac{\partial N_e}{\partial t} = -\gamma_s N_e^3, \quad (1)$$

subjected to $N_e(t=0) = (1-R)F/(hv\delta_e)$, where R is the reflectivity of the surface, F and hv are the incident fluence and photon energy, respectively, γ_s we define as the Auger recombination coefficient near the surface ($\text{cm}^6 \text{s}^{-1}$), and t is the time. For this analysis, $N_e(t=0)$ for the low and high repetition rate experiments are 5×10^{19} and $6 \times 10^{17} \text{ cm}^{-3}$, respectively. In Eq. (1), we assume that the only process affecting the change in number density in the conduction band is Auger recombination, which, here, we define as a surface process that is different than the bulk Auger recombination process. The solution to Eq. (1) is given by

$$N_e(t) = \left[\left(\frac{hv\delta_e}{(R-1)F} \right)^2 + 2\gamma_s t \right]^{-1/2}. \quad (2)$$

The number density is then related to the reflectivity through the Drude model, given by

$$\varepsilon = 1 - \frac{\omega_p^2}{\omega(\omega + i\tau_e^{-1})}, \quad (3)$$

where ω is the angular frequency of the incident photons, ω_p is the plasma frequency given by $\omega_p^2 = 4\pi N_e e^2 / m^*$, where e is the fundamental charge and m^* is the reduced effective mass for electrons and holes ($m^* = 0.12m_e$ where m_e is the free electron rest mass),¹³ and τ_e is the electron collisional frequency, which we take as ~ 100 fs for Si (effectively instantaneous over the time scale of interest).¹⁰ Given that $n+ik = \sqrt{\varepsilon}$, the normalized thermoreflectance signal is given by²³

$$\frac{\Delta R}{R} = \frac{\frac{[n(t+\Delta t) - 1]^2 + k^2(t+\Delta t)}{[n(t+\Delta t) + 1]^2 + k^2(t+\Delta t)}}{\frac{[n(t) - 1]^2 + k^2(t)}{[n(t) + 1]^2 + k^2(t)}}, \quad (4)$$

where t is the time, which we take as a reference at $t=0$, and Δt is the time after pulse absorption. Since we are only concerned with processes involving electrons leaving the conduction band, we scale the model to the experimental data at $t=30$ ps to avoid any complications from electron-phonon scattering and ambipolar diffusion.

Figure 3 shows the thermoreflectance model [Eq. (4)] fit to sample experimental data from Figs. 1 and 2. We only show one data set fit from each experimental setup since the various measurements on the samples were similar (within the experimental noise) when normalized at the peak (see Figs. 1 and 2), and the reported value of γ_s in the figure is based on the fit to the one depicted data set. The (pump) reflectivity, extinction coefficient, and excitation depth for Si at 400 and 785 nm are $R=0.484$ and $0.33 \mu\text{m}$, $k=0.521$ and $0.007 \mu\text{m}$, and $\delta_e=0.06$ and $8.92 \mu\text{m}$, respectively.²⁴ In the low repetition rate measurements, the average γ_s among the various measurements on the samples is $3.88 \times 10^{-30} \pm 0.92 \text{ cm}^6 \text{ s}^{-1}$. The high repetition rate measurements, however, exhibited a much higher Auger recombination coefficient, yielding an average value of $5.35 \times 10^{-28} \pm 0.08 \text{ cm}^6 \text{ s}^{-1}$.

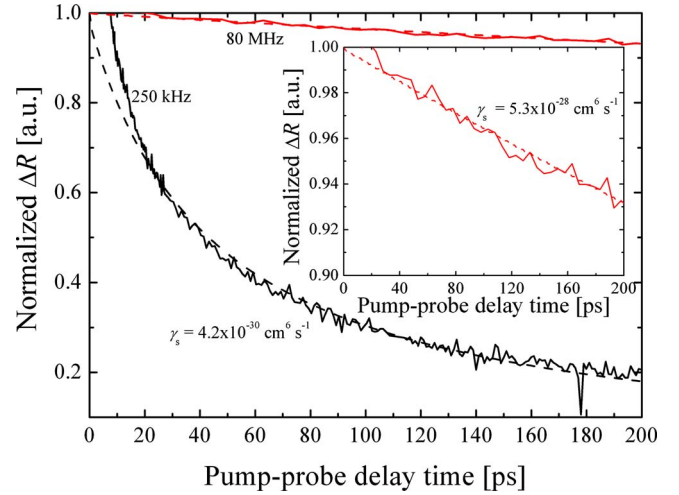


FIG. 3. (Color online) Thermoreflectance model fit to sample experimental data from the high and low repetition rate measurements. In the low repetition rate measurements, the average γ_s among the various measurements on the samples was determined as $3.88 \times 10^{-30} \pm 0.92 \text{ cm}^6 \text{ s}^{-1}$. The high repetition rate measurements, however, exhibited a much higher Auger recombination coefficient, yielding an average value of $5.35 \times 10^{-28} \pm 0.08 \text{ cm}^6 \text{ s}^{-1}$.

Auger recombination coefficients in Si have been measured to span the range from 10^{-31} to $10^{-30} \text{ cm}^6 \text{ s}^{-1}$.^{18,25,26} The Auger recombination coefficient determined from the low repetition rate data agrees well with the previously reported range of data; the slightly high value could be due to the surface treatments on the Si wafers. The high repetition rate data, however, yield an average best fit value for γ_s that is two to three orders of magnitude higher than literature values for Si. In the analysis of the data using Eq. (1), the initial excited carrier density is estimated by assuming that the number of carriers in the conduction band driving the thermoreflectance decay is that excited by a single pump pulse. However, since the Auger recombination time in Si in the low perturbative limit is longer than the time between pulses (and also longer than the time between pulse envelopes produced by the EOM modulating the pump pulse train at 11 MHz), the excited carriers in the conduction band will accumulate until the conduction band is saturated in the energy range of the incident pump laser pulse. Qualitatively, this explains why ΔR is much higher in the high repetition rate data compared to the low repetition rate data; the conduction band states are all filled in the laser energy range in the higher repetition rate data so incident photons cannot be absorbed. This means that the excited number density that drives the Auger decay will be much higher than that excited by a single laser pulse ($N_e \sim 6.0 \times 10^{17} \text{ cm}^{-3}$ as previously stated).

To estimate the excited number density in 80 MHz data, we assume that the conduction band states in Si are completely filled in an energy range of $hv - E_g$ above the conduction band minimum, where E_g is the band gap. Assuming a negligible increase in conduction band number density due to Fermi smearing, since we assume an unperturbed state at room temperature, the number of excited electrons in the conduction band due to pulse accumulation in the 80 MHz measurements is estimated by²⁷

$$N_e(t=0) = \frac{16\sqrt{2}\pi m^*}{3h^3} (hv - E_g)^{3/2} = N_{e,\text{sat}}, \quad (5)$$

where Eq. (5) assumes a parabolic conduction band and h is Planck's constant. Using Eq. (5), the excited number density in Si from 785 nm pulses is $5.8 \times 10^{19} \text{ cm}^{-3}$. Using this saturated excited number density in the thermoreflectance model yields an average best fit $\gamma_s = 5.45 \times 10^{-32} \pm 0.8 \text{ cm}^6 \text{ s}^{-1}$. This value is in better agreement with the literature value for the recombination coefficient in Si than γ_s determined assuming an excited number density from only a single pump pulse, however, is still relatively low compared to γ_s measured with the low repetition rate setup.

The lower value of γ_s determined from the high repetition rate measurements with Eq. (5) than that determined from the low repetition rate measurements could be due to the excited carrier number density assumption used in the reflectivity calculations. Equation (5) assumes that all empty states in the conduction band within the laser energy excitation range will be filled; this is effectively an upper limit for the excited number density. However, this may not be the case as there may be some of the electron population in the conduction band that recombines via Auger processes before the next pulse is absorbed. With a single measurement, both γ_s and N_e are difficult to determine. However, given both low and high repetition rate measurements, γ_s can be determined from the low repetition rate measurements without complication from pulse accumulation, and then the excited number density can be determined from the high repetition rate data by fitting the thermoreflectance model to the data by iterating N_e . Assuming $\gamma_s = 3.88 \times 10^{-30} \text{ cm}^6 \text{ s}^{-1}$ as determined from the low repetition rate measurements, the excited number density in the conduction band from the 785 nm pump pulse excitation is $6.5 \times 10^{18} \pm 0.4 \text{ cm}^{-3}$. We can also estimate the total excited number density including accumulation by examining the thermoreflectance signal of the high repetition rate data before and after zero pump-probe delay time. In the postprocessed high repetition rate data in Fig. 2, we subtract off the background signal to just examine the magnitude of the decay, as per the data correction procedure discussed by Stevens *et al.*²² However, examining the raw data before data processing shows that the average peak value of ΔR is ~ 10 and the average value before $t=0$ is ~ 1.5 ; a representative noncorrected data set from the high repetition rate experiment is shown in inset 2 of Fig. 2. Given that the lock-in amplifier measures the average thermoreflectance decay triggered to the 11 MHz repetition rate, the peak represents the total excited number density from all the pulses in the modulation envelope; for an 80 MHz oscillator being modulated at 11 MHz, this corresponds to ~ 4 pulses so the peak thermoreflectance at a value of ~ 10 corresponds to a total excited carrier density of $\sim 2.5 \times 10^{18} \text{ cm}^{-3}$. Therefore, the before zero time thermoreflectance value of ~ 1.5 corresponds to a residual number density of $\sim 0.5 \times 10^{18} \text{ cm}^{-3}$. This leads to an estimate of the excited carrier density of $\sim 3 \times 10^{18} \text{ cm}^{-3}$ from simple arguments by examining the measured signal. Although this method is very approximate, it gives order of magnitude agreement with N_e determined from the model fit procedure

discussed earlier ($6.5 \times 10^{18} \pm 0.4 \text{ cm}^{-3}$). In either case, these excited carrier densities are nearly an order of magnitude less than the saturated excited number density determined via Eq. (5), indicating that the 785 nm excitations at 80 MHz and 2 J m^{-2} incident fluence does not saturate the conduction band, so the Auger recombination coefficients at the surface of the Si wafers are slightly higher than literature values for bulk, nontreated Si.

IV. CONCLUSIONS

In summary, this work reports measurements of the Auger recombination coefficients of surface treated Si wafers measured from thermoreflectance decay using pump-probe experiments operating at two different repetition rates, 250 kHz and 80 MHz. The thermoreflectance signals measured with the two setups are drastically different, which is ascribed to the excited carrier density in the conduction band. In the low repetition rate case, the excited carriers recombine via Auger processes before the next pump excitation is absorbed. However, in the high repetition rate case, the rate in which the pump excitations are absorbed at the sample surface is higher than the Auger recombination rate, indicating that the excited carrier density in the high repetition rate experiments are much higher than in the low repetition rate measurements, even though the pump fluences are comparable. This is quantified with a coupled rate equation and thermoreflectance model fit to the experimental data.

ACKNOWLEDGMENTS

P.E.H. is grateful for funding from the LDRD program office through the Sandia National Laboratories Harry S. Truman Fellowship. Sandia is a multiprogram laboratory operated by Sandia Corporation, a Lockheed-Martin Co., for the United States Department of Energy's National Nuclear Security Administration under Contract No. DE-AC04-94AL85000.

- ¹A. Othonos, *J. Appl. Phys.* **83**, 1789 (1998).
- ²E. J. Yoffa, *Phys. Rev. B* **21**, 2415 (1980).
- ³A. J. Sabbah and D. M. Riffe, *Phys. Rev. B* **66**, 165217 (2002).
- ⁴T. Sjodin, H. Petek, and H.-L. Dai, *Phys. Rev. Lett.* **81**, 5664 (1998).
- ⁵E. Lioudakis, A. Othonos, E. Lliopoulos, K. Tsagaraki, and A. Georgakilas, *J. Appl. Phys.* **102**, 073104 (2007).
- ⁶E. Lioudakis, A. Othonos, and A. G. Nassiopoulou, *Appl. Phys. Lett.* **88**, 181107 (2006).
- ⁷A. Chin, K.-Y. Lee, B. C. Lin, and S. Horng, *Appl. Phys. Lett.* **69**, 653 (1996).
- ⁸J. Michael Klopff and P. M. Norris, *Int. J. Thermophys.* **26**, 127 (2005).
- ⁹J. M. Klopff and P. M. Norris, *Appl. Surf. Sci.* **253**, 6305 (2007).
- ¹⁰A. J. Sabbah and D. M. Riffe, *J. Appl. Phys.* **88**, 6954 (2000).
- ¹¹Y. Kostoulas, L. J. Waxer, I. A. Walmsley, G. W. Wicks, and P. M. Fauchet, *Appl. Phys. Lett.* **66**, 1821 (1995).
- ¹²V. Malyutenko and S. Chyrchuk, *Appl. Phys. Lett.* **89**, 051909 (2006).
- ¹³O. B. Wright and V. E. Gusev, *Appl. Phys. Lett.* **66**, 1190 (1995).
- ¹⁴P. Y. Yu and M. Cardona, *Fundamentals of Semiconductors: Physics and Materials Properties* (Springer, Berlin, 2005).
- ¹⁵P. E. Hopkins, J. M. Klopff, and P. M. Norris, *Appl. Opt.* **46**, 2076 (2007).
- ¹⁶C. K. Sun, F. Vallee, L. Acioli, E. P. Ippen, and J. G. Fujimoto, *Phys. Rev. B* **50**, 15337 (1994).
- ¹⁷H. M. van Driel, *Phys. Rev. B* **35**, 8166 (1987).
- ¹⁸C.-M. Li, T. Sjodin, and H.-L. Dai, *Phys. Rev. B* **56**, 15252 (1997).
- ¹⁹S. M. George, A. W. Ott, and J. W. Klaus, *J. Phys. Chem.* **100**, 13121 (1996).
- ²⁰P. E. Hopkins, J. R. Serrano, L. M. Phinney, S. P. Kearney, T. W. Grasser,

- and C. T. Harris, ASME J. Heat Transfer (in press).
- ²¹A. Brodeur and S. L. Chin, *J. Opt. Soc. Am. B* **16**, 637 (1999).
- ²²R. J. Stevens, A. N. Smith, and P. M. Norris, *Rev. Sci. Instrum.* **77**, 084901 (2006).
- ²³P. E. Hopkins, *J. Appl. Phys.* **105**, 093517 (2009).
- ²⁴E. D. Palik, *Handbook of Optical Constants of Solids* (Academic, Orlando, 1985).
- ²⁵K. G. Svantesson and N. G. Nilsson, *J. Phys. C* **12**, 5111 (1979).
- ²⁶W. Gerlach, H. Schlangenotto, and H. Maeder, *Phys. Status Solidi A* **13**, 277 (1972).
- ²⁷G. Chen, *Nanoscale Energy Transport and Conversion: A Parallel Treatment of Electrons, Molecules, Phonons, and Photons* (Oxford University Press, New York, 2005).